# PHOTORECEPTOR DEGENERATION AND ABNORMAL RETINAL VASCULOGENESIS

By

Matthew Nguyen

A Thesis Submitted to the Faculty of

The Charles E. Schmidt College of Medicine

In Partial Fulfillment of the Requirements for the Degree of

Master of Science

Florida Atlantic University

Boca Raton, FL

December 2021

PHOTORECEPTOR DEGENERATION AND ABNORMAL RETINAL

VASCULOGENESIS

by

Matthew Nguyen

This thesis was prepared under the direction of the candidate's thesis advisor, Dr. Wen Shen, Department of Biomedical Science, and has been approved by all members of the supervisory committee. It was submitted to the faculty of the Charles E. Schmidt College of Medicine and was accepted in partial fulfillment of the requirements for the degree of Master of Science.

SUPERVISORY COMMITTEE:

Wen Shen (Oct 26, 2021 10:22 EDT)

Wen Shen, Ph.D.
Thesis Advisor

Howard M. Prentice
Howard M. Prentice (Oct 26, 2021 10:37 EDT)

Howard Prentice, Ph.D.

Xupei Huang
Xupei Huang (Oct 26, 2021 12:1[illegible] EDT)

Xupei Huang, M.D., Ph.D.

Janet Robishaw, Ph.D.
Chair, Department of Biomedical Science

Sarah Wood
Sarah Wood (Oct 29, 2021 12:20 EDT)

Sarah Wood, M.D.
Interim Dean, Charles E. Schmidt College of Medicine

Robert W. Stackman Jr., Ph.D.
Dean, Graduate College

October 29, 2021
Date

ACKNOWLEDGEMENTS

I would like to express my sincerest gratitude to my thesis committee members, Dr. Xupei Huang and Dr. Howard Prentice, for their support and feedback throughout the process of writing this manuscript. I would like to especially thank my advisor, Dr. Wen Shen, for her continued guidance, understanding, and optimism. I will always be grateful for the chance she gave me as a young and inexperienced scholar. My life would not be the same had I not been a part of the Shen lab at the Charles E. Schmidt College of Medicine.

ABSTRACT

Author: Matthew Nguyen

Title: Photoreceptor Degeneration and Abnormal Retinal Vasculogenesis

Institution: Florida Atlantic University

Thesis Advisor: Dr. Wen Shen

Degree: Master of Science

Year: 2021

Abnormal vasculature in the retina, specifically tortuous blood vessels, are common to many of the most prevalent retinal degenerative diseases currently affecting millions across the world. The mechanisms of their formation and development in the context of retinal degenerative disease, however, are still poorly understood. The *rd1* and *rd10* mice are relatively well-studied animal models of retinal degenerative disease, however, there lacks a systematic characterization of vascular changes co-related to photoreceptor degeneration in the *rd1* and *rd10* retina. Here, we utilize advancements in confocal microscopy, immunohistochemistry, and image analysis software in order to systematically characterize vascular changes before and after retinal development in the *rd1* and *rd10* mice. We show that there are plexus specific changes in the retinal vasculature that parallel photoreceptor degeneration. Such information will be of

particular use to future studies investigating the role of vascular changes in retinal degenerative disease therapies.

# DEDICATION

This thesis is dedicated to my family who have ceaselessly supported me and encouraged me to take the path less traveled. I would like to particularly thank my parents, Tru and Nhi Nguyen, for fighting the obstacles of immigration in the hopes that their children would have greater opportunities, and my baby brother, Noah Nguyen, for making me believe that the future is in great hands.

I also dedicate this work to the great individuals that I am honored to call my closest friends. I give immense thanks to Gaby Rose for countless reviews of this thesis and for being my role model in all things academic or otherwise. I would like to thank Claude Gassant for many late nights and for reminding me that there is always a reason to laugh. I would also like to thank Ollivier Gassant for reminding me of where I came from and for inspiring me to continue in the face of adversity. Gaby, Claude, and Ollivier have always pushed me to go beyond and have instilled the “Plus Ultra” mentality in everything I do.

Last but not least, I would like to dedicate this thesis to my late mentor, Dr. Ira Gelb, and his great friend, Dr. Charlie Hennekens, for taking me under their wing and showing me how medicine is meant to be practiced and taught. It is my hope that I will become even half as good of a physician as Dr. Gelb and Dr. Hennekens.

PHOTORECEPTOR DEGENERATION AND ABNORMAL RETINAL VASCULOGENESIS

LIST OF TABLES ..... x

LIST OF FIGURES ..... xi

INTRODUCTION ..... 1

The Retinal Vasculature System in Development and Adulthood ..... 3

The *rd1* Mouse ..... 6

The *rd10* Mouse ..... 8

Advantages of Computer Modeling and Three-Dimensional Imaging Approaches ..... 10

METHODS ..... 13

Animals ..... 13

Immunohistochemistry ..... 13

Three-Dimensional Reconstruction of Vasculature and Statistical Analysis ..... 14

RESULTS ..... 16

Abnormal Vascular Development in the *rd1* Mouse ..... 16

Pathological Vascular Structure in the Adult *rd1* Retina ..... 19

Pathological Changes of Vasculature in the *rd10* mouse ..... 22

Statistical Analyses of Vascular Degenerative Patterns ..... 23

DISCUSSION ..... 31

Photoreceptor Degeneration Influences Vascular Development in RD Mice ..... 31

Statistical Analyses of Vasculature in Developing and Adult *rd1* and *rd10* Retina ..... 33

Conclusion ..... 35

Future Perspectives ..... 35

REFERENCES ..... 37

LIST OF TABLES

Table 1. Comparison of means of the following averaged parameters in imaging analysis of the retinal trilaminar vascular network in wild-type (WT) mice: vascular area fraction, number of branches, number of junctions, and junction to branch ratio. WT: n=9, regions of interest defined at 250 μm$^2$, age: 4W. SP: Superficial Plexus, IP: Intermediate Plexus, DP: Deep Plexus. ..... 27

Table 2. Comparison of means of the following averaged parameters in imaging analysis of the retinal trilaminar vascular network in *rd1* mice: vascular area fraction, number of branches, number of junctions, and junction to branch ratio. *rd1*: n=9, regions of interest defined at 250 μm$^2$, age: 8W. SP: Superficial Plexus, IP: Intermediate Plexus, DP: Deep Plexus. ..... 28

Table 3. Comparison of means of the following averaged parameters in imaging analysis of the retinal trilaminar vascular network in *rd10* mice: vascular area fraction, number of branches, number of junctions, and junction to branch ratio. *rd10*: n=9, regions of interest defined at 250 μm$^2$, age: 8W. SP: Superficial Plexus, IP: Intermediate Plexus, DP: Deep Plexus. ..... 29

LIST OF FIGURES

Figure 1. (a) A diagram of a cross-section of the eye showing the anatomy and relative location of the retina, (b) The organization of neural structure and blood vessels in a cross section of the retina. RPE: retinal pigment epithelium; IS/OS: inner segment/outer segment; ONL: outer nuclear layer; OPL: outer plexiform layer; INL: inner nuclear layer; IPL: inner plexiform layer; GCL: ganglion cell layer.... 3

Figure 2. Vascular development in the mouse retina. (a) Three-dimensional view of infiltrating vasculature forming the superficial, intermediate, and deep plexus of the retina. (b) Spread of vasculature from the center retina to the middle and peripheral regions during retinal development. ..... 6

Figure 3. Early onset rod degeneration in the FVB/N mouse. The FVB/N strain carries a naturally occurring pde6b gene mutation similar to the rd1 mouse. (a) The anti-rhodopsin labeling (red) of rod outer segments and DAPI counterstaining of the cell nuclei (blue) in retinal cross sections of FVB/N mice at various postnatal ages. By p14 the FVB/N retina has lost a significant number of rods and the retina is thinner than normal, there is a further loss at p21. Apposition of the RPE and the surviving neurons are stained by DAPI at p28, and at p35 where there is no rhodopsin labeling. (b) Anti-rhodopsin labeling in control retinal sections at the age of p35 displays robust staining throughout the layer of outer segments (OS). (c) The thicknesses of the ONL and INL measured from control and FVB/N

retinal sections shows a progressive reduction in FVB/N retinas. Scale bar, 20μm. (Adapted from Yang et al. 2015, PLoS ONE.) ..... 8

Figure 4. A significant amount of photoreceptor cells are present in the rd10 retina at postnatal day 39. The retinal cross-sections were labeled by anti-M-opsin and anti-S- opsin molecules (red) and counter stained with a nuclear dye, DAPI (blue), showing that a significant amount of photoreceptor nuclei are present in the retinal tissue. (Adapted from Li et al. 2019, Experimental Eye Research.) ..... 10

Figure 5. Abnormal vascular development in the *rd1* retina. (a) Vascular staining with fluorescent marker against anti-CD31 at p7 in rd1 and wild-type mice showing normal development of the superficial vascular plexus. Scale bars: 25 μm (left), 50 μm (right) (b) Vascular staining with fluorescent markers against anti-CD144 at p14 depicting loss of blood vessels in the intermediate and deep plexus of the *rd1* mouse retina. Scale bars: 25 μm (left), 50 μm (right) (c) Vascular staining with fluorescent markers against anti-CD31 at p21 depicting near total loss of blood vessels in the intermediate and deep plexus of the *rd1* retina compared to the wild-type control. Scale bars: 25 μm (d) Retinal cross sections of the wild-type and *rd1* mouse at p14 with anti-GFAP staining showing minimal expression in the wild-type and increased expression in the *rd1* retina..... 18

Figure 6. Immuno-labeling and confocal imaging of vascular endothelial cadherin by anti-CD144 in flat-mounted retinas depicted structures of blood vessels in the adult mouse retinas from (a) 5-month-old healthy wild-type (WT) and (b) photoreceptor degenerated (*rd1*) mice. Top panels: superficial plexuses of the WT and *rd1* retinas (left) and constricted z-stack images of cross-section of the retinas

(right). Loss of blood vessels at the intermediate and deep vasculature layers of the *rd1* mouse retina indicated by the absence of green, fluorescent labeling in the three plexuses (middle panels). Images in the bottom row show angiographic changes in the retinal vasculature as a superimposition of the superficial, intermediate, and deep plexuses in (c) 5-month-old WT mice and (d) 5-month-old *rd1* mice. ..... 20

Figure 7. Loss of rod photoreceptor cells and significant increase of GFAP expression in the *rd1* mouse. Immuno-labeling with anti-Rho (red) and anti-GFAP (red), counter-staining with a nuclei dye DAPI (blue) in cross-sections of (a) wild-type retina and (b) the *rd1* retina. ..... 22

Figure 8. Confocal images of the superficial, intermediate, and deep plexuses of wild-type, *rd1*, and *rd10* mice at four weeks postnatal. ..... 23

# INTRODUCTION

The retina, being primarily responsible for vision, receives light and converts the light signals into neural signals and sends these signals on to the brain for high visual perception. Retinal degenerative diseases are debilitating conditions with huge impacts on quality of life. Diseases characterized by retinal degeneration, such as retinitis pigmentosa, have high incidences of blindness in afflicted patients caused by the death of the light-detecting photoreceptor cells in the retina[1,2]. Given the severity and impact of these diseases, more information on the pathogenesis of retinal degeneration is urgently required. The retinal degenerative (RD) mouse models, the *rd1* and *rd10* mice, have been established as relatively well-studied animal models of retinal degeneration; however, there is much left to be understood concerning the nature of these diseases. Retinal degeneration typically begins with the loss of rod photoreceptor cells in the retina, followed by the loss of the cones. Without these cells the phototransduction cascade, a molecular signaling pathway that involves the detection and conversion of light stimuli into an electrical signal, is not possible and, therefore, progressive vision loss is observed often degrading into total blindness.

The retina is the innermost layer of tissue lining the back of the eye and is composed of various neural cells and an intricate network of blood vessels (See Fig. 1a and 1b). In brief, there are five classes of retinal neurons: photoreceptors (including rods and cones), horizontal, bipolar, amacrine and ganglion cells. The neural structure of the

retina is composed of three nuclear layers: photoreceptors in the outer nuclear layer (ONL), horizontal, bipolar and amacrine cells located in the inner nuclear layer (INL), and the ganglion cell layer (GCL). The cells are communicating within two synaptic layers: outer plexiform layer (OPL) and inner plexiform layer (IPL) in the distal and proximal retina respectively. Light enters the eye, passes through the cornea, lens and vitreous and finally reaches the photoreceptors of the retina (see Fig. 1a). Light activates these photoreceptors where light signals are converted into electrical and chemical signals and are then processed by horizontal, bipolar, and amacrine cells in the OPL and IPL. Ultimately, the visual signals reach the ganglion cells that send the information to the brain via optic nerves.

The vascular and nervous systems, two major networks in the mammalian retina, show a high degree of anatomical parallelism and functional crosstalk (see Fig. 1b). During development, neurons guide and attract blood vessels, and consequently this parallelism is established. Indeed, disruptions to the activity of the retinal neural cells can lead to devastating changes in the organization and proliferation of the retinal vasculature.

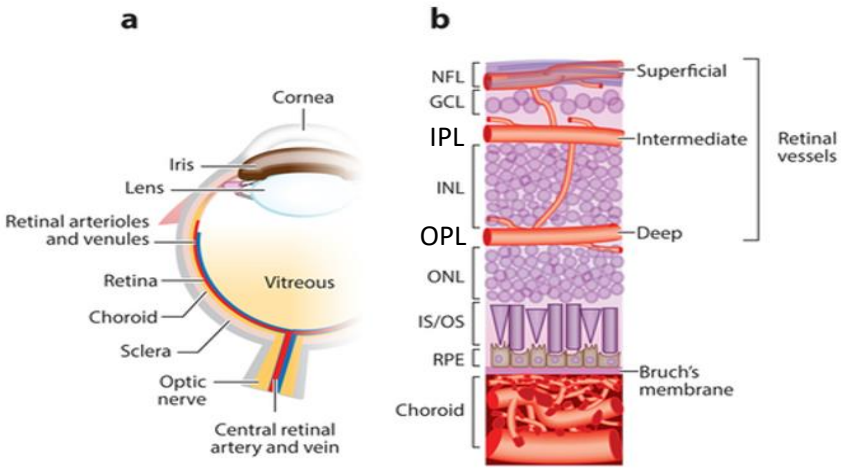


**Figure 1. (a)** A diagram of a cross-section of the eye showing the anatomy and relative location of the retina, **(b)** The organization of neural structure and blood vessels in a cross section of the retina. RPE: retinal pigment epithelium; IS/OS: inner segment/outer segment; ONL: outer nuclear layer; OPL: outer plexiform layer; INL: inner nuclear layer; IPL: inner plexiform layer; GCL: ganglion cell layer.

## The Retinal Vasculature System in Development and Adulthood

Distinct from humans, the development of retinal blood vessels in mice is postnatal and occurs layer by layer in a trilaminar network. The trilaminar retinal vascular network branches off the central retinal artery after birth, making up the superficial plexus in the nerve fiber layer, the intermediate plexus on top of the inner nuclear layer, and the deep plexus on the other side of the inner nuclear layer[5] (see Fig. 2a and 2b). This postnatal development allows for ease of study in analyzing vascular growth and changes as they relate to retinal development and degeneration.

In general, the processes by which vascular networks are formed are referred to as vasculogenesis and angiogenesis. The formation of vasculature and major vessels are typically initiated by the process of vasculogenesis where precursor angioblast cells differentiate into the endothelial cells that compose the vessel. This process is then followed by angiogenesis where existing endothelial cells form the remainder of the

vasculature by the processes of splitting and extending[6]. Actually, it has been well documented that the development of the primary vasculature in the retinal trilaminar network is accomplished through vasculogenesis rather than angiogenesis[6,7].

In mice, the formation of each plexus in the trilaminar network occurs in a time specific manner beginning with the initial formation of the superficial vascular plexus in the nerve fiber layer occurring in the first ten days after birth (see Fig. 2a). Vessels from the superficial plexus then infiltrate below the inner nuclear layer and begin the process of forming the deep vascular plexus in the distal retina typically between postnatal day eight and twelve. Around postnatal day fourteen, vessels will begin infiltrating from the deep plexus back to the surface of the inner nuclear layer in the inner retina to form the intermediate vascular plexus. Extension of the vascular plexuses from the central retina to the middle and peripheral regions is typically accomplished after the second week after birth (see Fig. 2b).

In the adult retina, this complex trilaminar network of vasculature is required to meet the high metabolic needs of neural tissue found in the retina. Any deviations from normal vascular development in the retina can have grave consequences for the function of such demanding tissues. It has also been documented that the pathogenesis of certain disease processes can occur through developmental or mechanical changes in one or more vascular plexuses[8,9,10]. Regarding the function of the retina, abnormal development or changes to the trilaminar vascular network interfere with the signal transduction of light into electrical-chemical signals in photoreceptors and neural synapses in the rest of the retina. The resulting effect is partial to full vision loss in the afflicted organism due to the degeneration of retinal cells such as the photoreceptors. Vascular changes resulting in

the suspension of the delivery of oxygen and nutrients to these cells with high metabolic demand leads to widespread degeneration of the retina. While in humans it is difficult to visualize changes in retinal vascular development due to the prenatal nature of the process, similar changes in mice are easily observed through a microscopy and imaging system. Mice are also particularly of use in studying such vascular changes as there is an abundance of genetic models of retinal degeneration available. This project studied the different patterns of retinal vascular degeneration in the popular retinal degenerative disease – retinitis pigmentosa. Two mouse models, the *rd1* and *rd10* mouse, were used in this study.

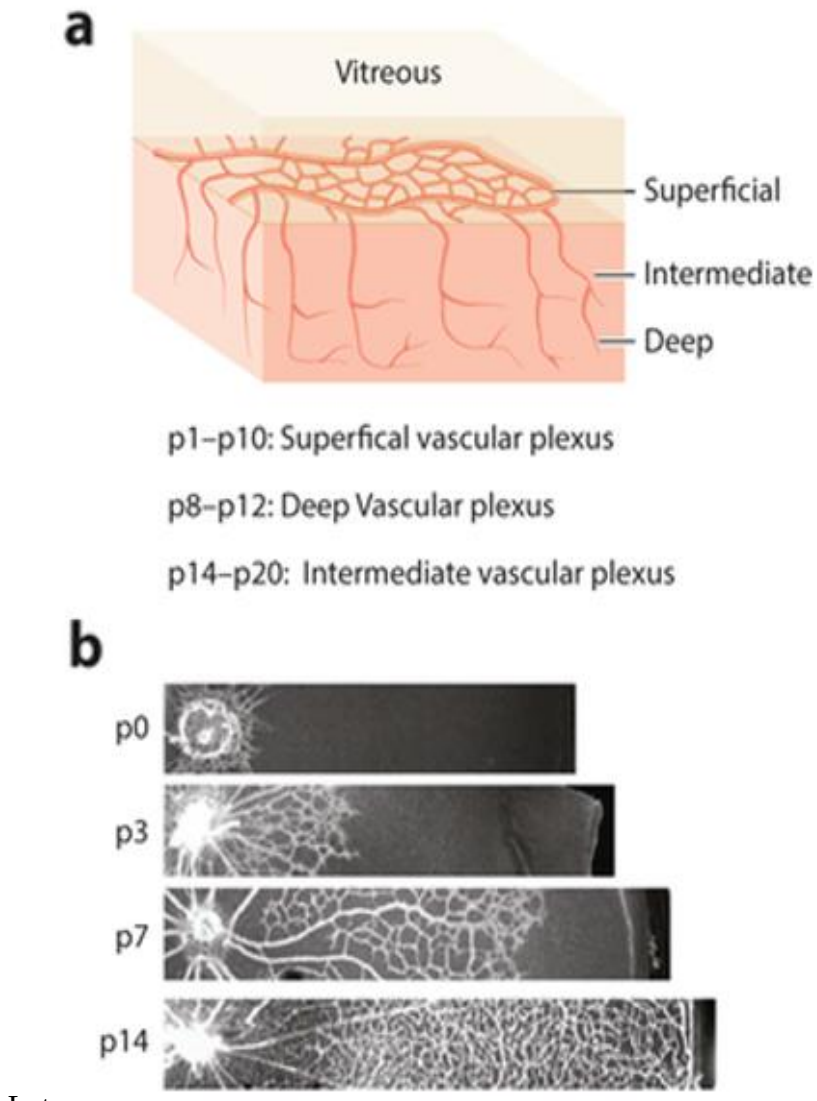


**Figure 2.** Vascular development in the mouse retina. **(a)** Three-dimensional view of infiltrating vasculature forming the superficial, intermediate, and deep plexus of the retina. **(b)** Spread of vasculature from the center retina to the middle and peripheral regions during retinal development.

## The *rd1* Mouse

The *rd1* mouse carries a nonsense mutation in the photoreceptor cGMP phosphodiesterase 6b (pde6b) gene which defectively encodes the beta subunit of rod phosphodiesterase, leading to severe retinal degeneration[11]. While gene therapies have

been extensively documented in the *rd1* mouse model, there is little that is understood concerning the nature of vascular changes characterizing retinal degeneration in this animal model[12,13].

The *rd1* mice are characterized as fast models of retinal degeneration, typically losing rod photoreceptor cells within the first weeks after birth which profoundly affects retinal development in the early stages. A representative study of photoreceptor degeneration and structural changes of the retina in the *rd1* mouse described the time frame of loss of opsin molecules contained by rod photoreceptor cells and thinning of the ONL and INL as seen in Figure 3a, 3b, and 3c[14]. The study using antibody labeling of rhodopsin molecules reported a progressive loss of rhodopsin beginning at p14 signifying the death of rod photoreceptors, with total loss of rhodopsin labeling at p35 in comparison to the healthy control (see red color, Fig. 3a and 3b). Figure 3c depicts the gradual thinning of the ONL and INL from p14 to 6 months in the FVB/N mouse that carries a naturally occurring mutation in the *pde6b* gene similar to *rd1* mice.

The early onset of retinal degeneration in the *rd1* mice make them ideal for repeated data collection, allowing for the comparison of multiple subjects and determination of consistent changes. Additionally, mutations in the same pde6b gene causing retinal degeneration in the *rd1* mouse have also been identified in human retinitis pigmentosa patients[15]. This makes the *rd1* mouse an ideal model to study the specific developmental and pathological changes that occur in certain human retinal degenerative diseases.

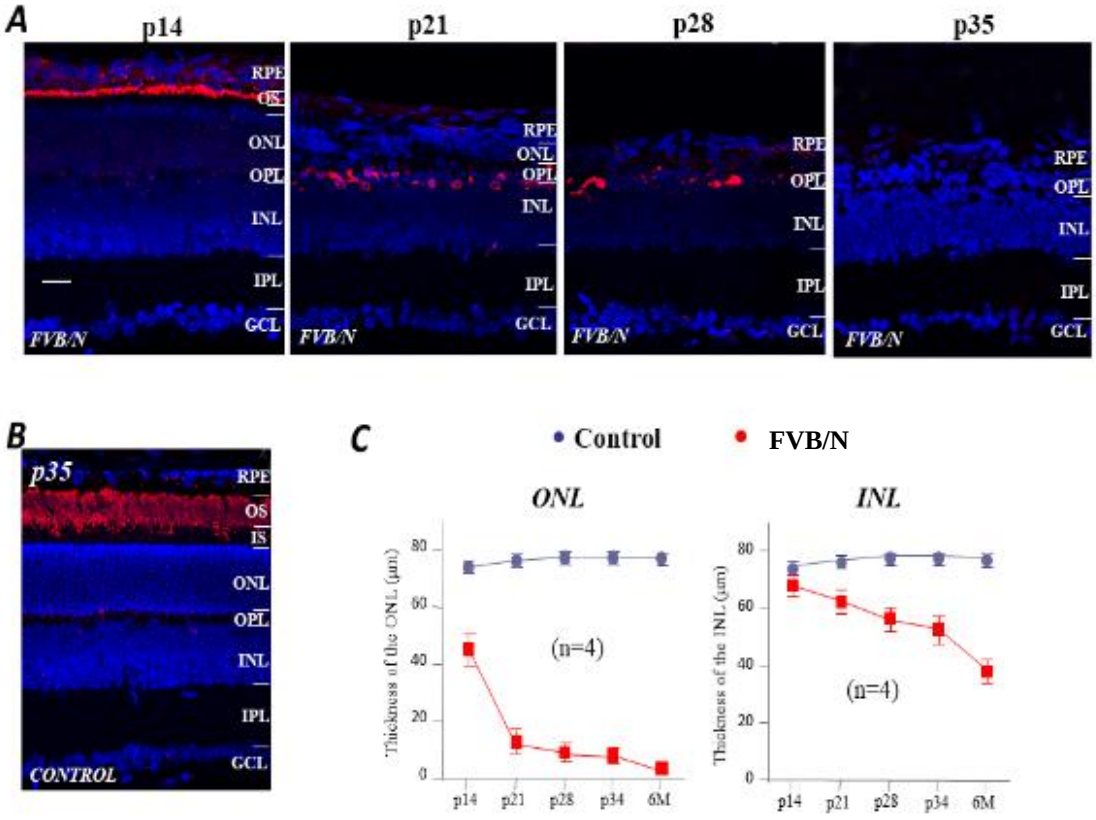


**Figure 3.** Early onset rod degeneration in the FVB/N mouse. The FVB/N strain carries a naturally occurring pde6b gene mutation similar to the rd1 mouse. **(a)** The anti-rhodopsin labeling (red) of rod outer segments and DAPI counterstaining of the cell nuclei (blue) in retinal cross sections of FVB/N mice at various postnatal ages. By p14 the FVB/N retina has lost a significant number of rods and the retina is thinner than normal, there is a further loss at p21. Apposition of the RPE and the surviving neurons are stained by DAPI at p28, and at p35 where there is no rhodopsin labeling. **(b)** Anti-rhodopsin labeling in control retinal sections at the age of p35 displays robust staining throughout the layer of outer segments (OS). **(c)** The thicknesses of the ONL and INL measured from control and FVB/N retinal sections shows a progressive reduction in FVB/N retinas. Scale bar, 20μm. (Adapted from Yang et al. 2015, PLoS ONE.)

By studying abnormal vascular development in the degenerative rd1 mouse retina, it can help us to better understand the relationship of photoreceptor and vascular development in physiological and pathological conditions.

## The *rd10* Mouse

Another popular mouse model is the *rd10* mouse, which is similar to the *rd1* mouse in that it also carries a mutation in the photoreceptor cGMP phosphodiesterase 6b

(pde6b) gene, however, the mutation in *rd10* mice occurs on exon 13 instead of exon 7 in *rd1* mice[16]. The result of this difference in genetics is shown in the slower onset of retinal degeneration in the *rd10* mouse in comparison to the *rd1* mouse in which the mutation occurs on exon 7. Retinal degeneration in the *rd1* mouse occurs within the first two weeks of postnatal life, whereas retinal degeneration in the *rd10* mouse does not occur until the fourth week after birth[17]. As shown in a previous study, even in the postnatal sixth weeks, significant amounts of photoreceptor cells are still present in both male and female rd10 mice (see Fig. 4, blue color, DAPI stained nuclei in the ONL), although the antibody labeling of M- and S-opsin molecules shows that the expression of opsins in photoreceptors are reduced in the *rd10* at this age (see red color, Fig. 4) suggesting that photoreceptors are undergoing degeneration[18].

The slower degeneration makes the *rd10* mouse an important model for studying neuronal and vascular degeneration after retinal development is completed since neuro-vascular development in the mouse retina is typically completed by the end of the third postnatal week. Since the severe degeneration of the retinal photoreceptors does not occur until after the development of the retinal vasculature is accomplished in *rd10* mice, this model allows us to study the time specific pathological changes of the retinal vascular network in the post-development and adult animals. Both the *rd1* and *rd10* mice serve as readily accessible models of photoreceptor degeneration and the pathological changes of the vascular system that accompany it.

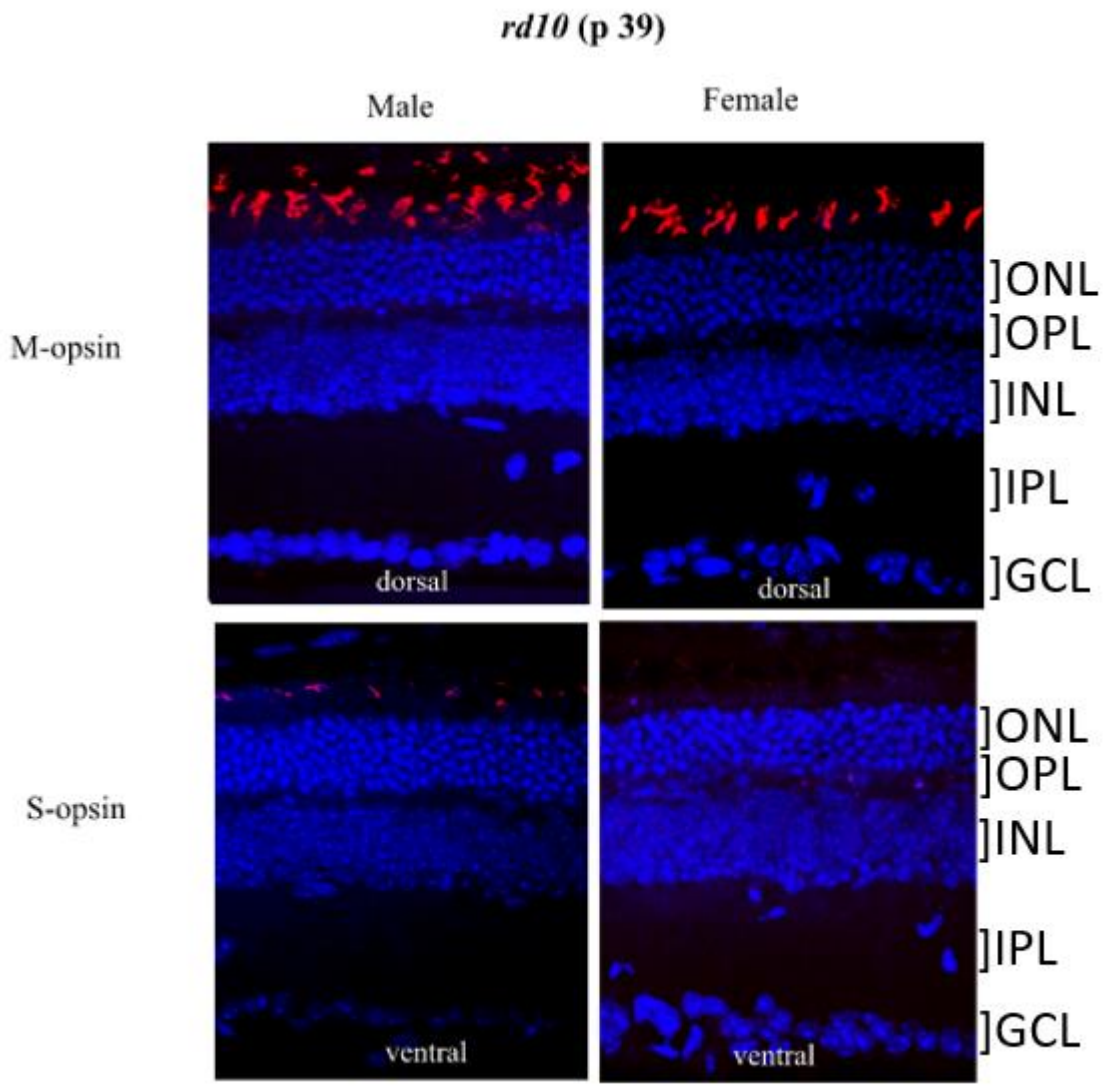


**Figure 4.** A significant amount of photoreceptor cells are present in the rd10 retina at postnatal day 39. The retinal cross-sections were labeled by anti-M-opsin and anti-S- opsin molecules (red) and counter stained with a nuclear dye, DAPI (blue), showing that a significant amount of photoreceptor nuclei are present in the retinal tissue. (Adapted from Li et al. 2019, Experimental Eye Research.)

## Advantages of Computer Modeling and Three-Dimensional Imaging Approaches

The ready availability of open-source imaging software combined with improvements to confocal laser scanning microscopy make studying of cellular and molecular structure changes of the rd1/rd10 mouse retina highly accessible. However, at

the current time there exists no systematic characterization of retinal vasculogenesis in the rd1/rd10 mouse retina with plexus-specific visualizations of the vasculature. In this study, we utilize immunohistochemical techniques combined with confocal imaging and open-source imaging and reconstruction software to depict the vascular changes that accompany photoreceptor degeneration in both *rd1* and *rd10* mouse models of retinal degeneration. Three-dimensional reconstructions of the retinal vasculature allow us to depict the fine structural changes of the vessels in wild-type and the degenerative retinas, circumventing the need for expensive or invasive methods of observation. As pointed out by Rust et al. the few systematic characterizations of retinal vasculogenesis available outside of the *rd1* mouse are difficult to compare due to inconsistencies within parameters[3]. In this study we use vascular area fraction, number of branches, number of junctions, and junction to branch ratio as parameters to systematically describe vascular changes in the retinal trilaminar network. By using biologically relevant parameters to characterize vascular changes, we provide visual insight and data for future studies into the RD mice and translation into clinical application.

It is important to note that the retinal trilaminar vascular network provides oxygen and nutrition to the highly sensitive neural cells that initiate the phototransduction cascade for vision perception. It has been well documented that vascular density is related to the metabolic demand of a certain tissue, higher demand is typically associated with greater vascular density which allows for the transfer of oxygen and nutrients to the tissue[4]. By visually depicting the vascular changes that occur in the rd1 and rd10 mouse models of retinal degeneration and systematically characterizing these changes using biologically relevant parameters related to vascular density, we offer important insight to

the short-term and long-term pathological changes that occur in retinal degenerative diseases such as retinitis pigmentosa. This body of work can serve as the basis for future studies aiming to rescue function in the retina with disease processes dependent upon or independent of vascular changes in the trilaminar network.

# METHODS

All described procedures involving live animals were approved by the Institutional Animal Care and Use Committee of Florida Atlantic University. The study was conducted in compliance with federal regulations and the ARVO Statement for the Use of Animals in Ophthalmic and Vision Research.

## Animals

The experiments performed in this study were centered on murine models of retinal degeneration, the *rd1* (*Pde6brd1*) mouse with FVB/N background and *rd10* (B6, CXB1-Pde6b rd10 /J) mouse strain with C57BL/6 background, and wild-type C57BL mice were purchased from the Jackson Laboratory (Bar Harbor, ME). Both strains were bred in house to produce the pups needed for the study. Monogamous breeder pairs of each strain and their offspring were housed in regular static microisolator cages under climate-controlled conditions, provided food and tap water ad libitum. The light cycle for the animals was set at a 12:12 h dim light/dark cycle. For rd10 mice, once pups were born, these cages were transferred to a dark cycle only using red light for husbandry duties (i.e., 15 min health checks daily and 1 h cage change per week) to mimic a dark condition for the mice.

## Immunohistochemistry

Retinal tissue was collected from wild-type and rd1/rd10 mice at various postnatal time points and stained with specific antibodies against retinal vascular proteins, VE-Cadherin (anti-CD144)- and PECAM-1 (anti-CD31). Freshly enucleated eyes were fixed for 20-30min in a phosphate buffered saline (PBS) solution containing 4% paraformaldehyde. After removing the corneas and lenses, the retinas were dissociated from paraformaldehyde fixed eyecup. The retinas were rinsed with 0.1% Tween and 0.3% Triton-X in PBS (PBST-T) solution, and then treated with a locking solution consisting of 10% goat or donkey serum in PBST-T solution for 1hr. They were then incubated in primary antibodies, either anti-CD144 or anti-CD31, dissolved in a mixture containing either 3% goat or donkey serum in PBST-T and held 72hrs at 4°C. Negative controls were performed with the same solutions but lacking the primary antibody. After three 15 min washes of the unbinding antibodies in the retinas with a PBST-T solution, the retinas were incubated with the secondary antibodies, Alexa 488- and Cy3-conjugated antibody (Jackson Immunoresearch, West Grove, PA) each at a concentration of 1:1000, for overnight at $4^{o}$ C. the retina were subsequently rinsed with PBST, mounted in Vectashield mounting medium (Vector Laboratories, Burlingame, CA) and viewed with a confocal laser-scanning microscope (LMS 700, Zeiss, Munich, Germany). Images were acquired with 10x, 20x, and 40x oil-immersion objectives, and processed with the Zeiss Microscope Software Zen.

**Three-Dimensional Reconstruction of Vasculature and Statistical Analysis**

Three-dimensional reconstructions of the trilaminar retinal vascular plexus network were rendered by compiling confocal image z-sections in the open-source ImageJ (FIJI) software. The image packs were then exported in raw format to the

ParaView Suite software where different perspectives of the models were recorded after rendering. The individual vascular layers of the trilaminar network were then systematically analyzed in FIJI for vascular area fraction using the built-in measurement and thresholding tools, and the number of junctions and number of branches using the analyze skeleton plugin. Each singular plexus layer was analyzed with the above-mentioned parameters at specific time points with multiple ROI defined at 250 $\mu m^2$ in the center, middle, and peripheral retina. Prior to analysis, the images were processed and converted into binary images. For branches and junctions, the binary images were converted into skeleton tracings of the vasculature. Means were then compared using the IBM SPSS software suite.

# RESULTS

We utilized two mouse models of retinal degenerative disease (*rd1* and *rd10*) in order to compare and depict the vascular changes occurring in either rapid photoreceptor degeneration or slower photoreceptor degeneration, respectively. The wild-type mice were used as controls in the imaging study.

## Abnormal Vascular Development in the *rd1* Mouse

In order to depict the vascular changes that occur during development in the wild-type and *rd1* mouse, we captured confocal microscopy images of the wild-type and *rd1* degenerative mouse retina at three postnatal time points: p7, p14, and p21. The primary antibodies against VE-Cadherin and PECAM-1, anti-CD144 and anti-CD31 proteins, and subsequent incubation with fluorescence-conjugated secondary antibodies (FITC or Cy3) were used as fluorescent markers to visualize the vasculature; both antibodies resulted in uniform vascular staining. Figure 5a shows that at p7, there is relatively normal development of the superficial vascular plexuses in both the wild-type and *rd1* mouse. Some growing vessels from the superficial layers extending towards the deep plexus can be seen passing through the intermediate plexus in the wild-type; however, this vascular developmental process is largely inhibited in the *rd1* retina (see Fig. 5a, middle and bottom panels in comparison of Wild-type and *rd1*).

At p14, there is a significant loss of the blood vessels in the intermediate and deep plexus of the *rd1* mouse retina compared to the wild-type control (see Fig. 5b). The result

suggests that due to an early onset of photoreceptor degeneration, it highly affects the vascular development at the early age of the *rd1* retina.

By p21 the intermediate and deep vascular plexuses of the *rd1* mouse retina are nearly devoid of any vasculature indicated by the absence of fluorescence labeling (see Fig. 5c, right). At p21 in the wild-type mouse retina, there is a developed plexus in all three layers, forming the trilaminar retinal vascular network (see Fig. 5c, left). Thus, we conclude that vascular development in the intermediate and deep plexuses of the *rd1* retina is ceased by rapid photoreceptor degeneration in this disease model.

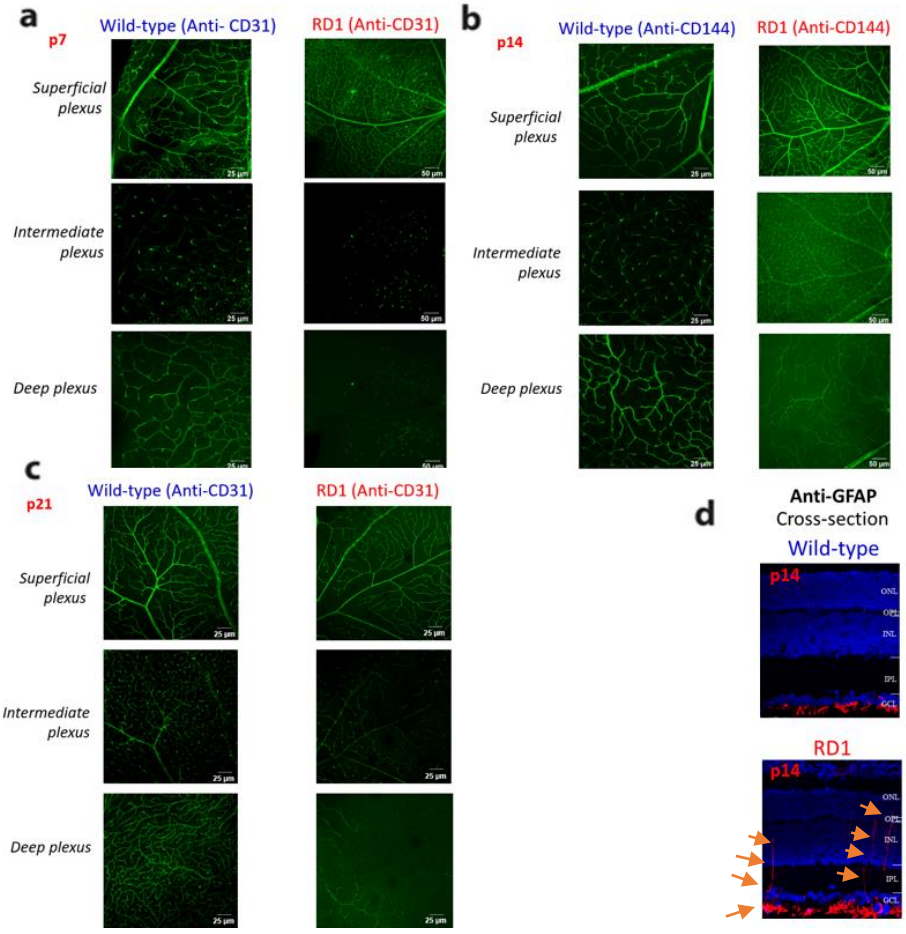


**Figure 5.** Abnormal vascular development in the *rd1* retina. **(a)** Vascular staining with fluorescent marker against anti-CD31 at p7 in rd1 and wild-type mice showing normal development of the superficial vascular

plexus. Scale bars: 25 µm (left), 50 µm (right) **(b)** Vascular staining with fluorescent markers against anti-CD144 at p14 depicting loss of blood vessels in the intermediate and deep plexus of the *rd1* mouse retina. Scale bars: 25 µm (left), 50 µm (right) **(c)** Vascular staining with fluorescent markers against anti-CD31 at p21 depicting near total loss of blood vessels in the intermediate and deep plexus of the *rd1* retina compared to the wild-type control. Scale bars: 25 µm **(d)** Retinal cross sections of the wild-type and *rd1* mouse at p14 with anti-GFAP staining showing minimal expression in the wild-type and increased expression in the *rd1* retina.

Photoreceptor degeneration in the *rd1* mouse is also accompanied by increased expression of glial fibrillary acidic protein (GFAP), a protein coding gene. GFAP is expressed by astrocytes and Muller cells[19]. It is known that both astrocytes and Muller cells have a close relationship with endothelial cells during retinal development. Previous studies have shown that GFAP expression largely increases in Muller cells in retina exhibiting photoreceptor degeneration[19,20,21]. Here, we used the antibody against GFAP (anti-GFAP) to detect pathological changes of GFAP expression at the early stage of photoreceptor degeneration in the *rd1* retina. As shown in Figure 5d, at p14 the expression of GFAP is observed in both the end-feet and fibers of Muller cells in a vertical section of the *rd1* retina (see arrows). When compared to the control, the expression is observed only in the end-feet of Muller cells in the wild-type retina. The overexpression of GFAP in the degenerative retina indicates that gliosis occurs as early as p14 days of retinal development in the *rd1* mouse.

**Pathological Vascular Structure in the Adult *rd1* Retina**

Initially, immunohistochemical labeling of retinal tissue from five-month-old wild-type and age-matched *rd1* mice with antibodies against anti-CD144 and fluorescent secondary antibodies (Alexa 488) confirmed that there were plexus-specific changes in the vasculature of the *rd1* mouse retina. Confocal imaging results depicted significant structural changes in the intermediate and deep plexuses in the *rd1* retina compared to the

age-matched wild-type control. The absence of green, fluorescent antibodies in the intermediate and deep vascular plexuses indicate a distinct loss of blood vessels in those layers (see Fig. 6a and 6b). Superimposition of the three vascular plexuses show that most of the vessels that persist in the adult rd1 retina originate from the superficial plexus (see Fig. 6c and 6d). These preliminary results demonstrated that angiographic changes and loss of blood vessels after development are critically involved in the progression of retinal degeneration in the *rd1* mouse. There is reason to believe that severe tortuosity in the distal retina, as evidenced by loss of blood vessels in the intermediate and deep vasculature layers, leads to ischemic attack and subsequent rod photoreceptor degeneration caused by the *pde6b* gene mutation.

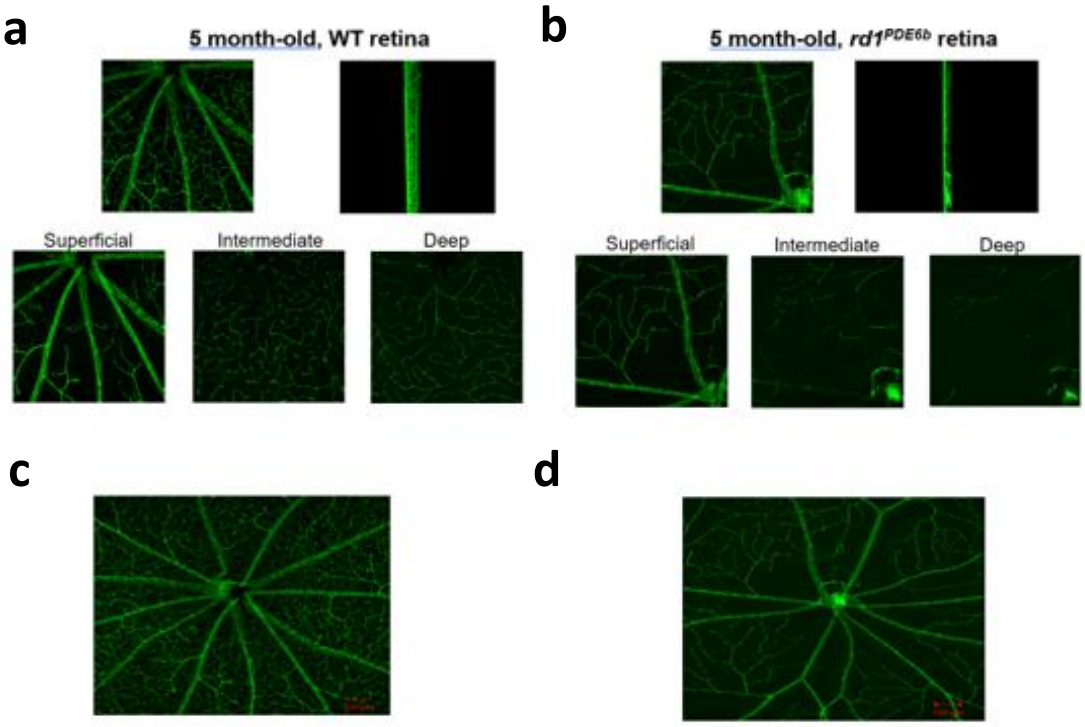


**Figure 6.** Immuno-labeling and confocal imaging of vascular endothelial cadherin by anti-CD144 in flat-mounted retinas depicted structures of blood vessels in the adult mouse retinas from **(a)** 5-month-old healthy wild-type (WT) and **(b)** photoreceptor degenerated (*rd1*) mice. Top panels: superficial plexuses of

the WT and *rd1* retinas (left) and constricted z-stack images of cross-section of the retinas (right). Loss of blood vessels at the intermediate and deep vasculature layers of the *rd1* mouse retina indicated by the absence of green, fluorescent labeling in the three plexuses (middle panels). Images in the bottom row show angiographic changes in the retinal vasculature as a superimposition of the superficial, intermediate, and deep plexuses in **(c)** 5-month-old WT mice and **(d)** 5-month-old *rd1* mice.

To demonstrate loss of photoreceptors in the adult *rd1* retina, we used the antibody specific for rhodopsin molecules (anti-Rho) that are expressed in rod photoreceptors and a nuclear dye, DAPI, labeling nuclei in the ONL. As shown in figure 7a and 7b, anti-Rho labeled the outer segments of rod photoreceptors in a cross-section of the wild-type retina, and the labeling was absent in the *rd1* retina (see Fig. 7a and 7b, red color in the left panels). The DAPI nuclear labeling of the retinal cross-section also indicates that there was a significant loss of neurons in the ONL evidencing that not only rods are degenerated, but cones are also completely degenerated in the *rd1* mice at the age of five months. The nuclear labeling results also indicate that the INL of the *rd1* retina is thinner compared to the wild-type, consistent with previous studies reporting that the loss of photoreceptors causes cell degeneration in the INL[14]. Therefore, we conclude that the loss blood vessels in the intermediate and deep plexuses are corresponded to loss of neurons in the ONL and INL during the disease progression in the *rd1* mouse.

The adult *rd1* mouse retina also demonstrated a great increase in GFAP expression as photoreceptor degeneration progressed in the retina in comparison to the age-matched wild-type mouse retina (see Fig. 7a and 7b red color in right panels). While the exact action of GFAP in this case is not fully understood, it is believed that GFAP is involved in the maintenance and movement of astrocytes, glial cells that aid in nerve conduction and stability[22]. The increased expression of GFAP may represent an attempt at preserving nerve conduction between the eye and brain in the absence of both

photoreceptor cells and vasculature. The most common type of glial cell found in the mouse and human retina are known as Muller cells. Interestingly muller cells, while functionally similar to astrocytes, express small amounts of GFAP under normal physiological conditions compared to astrocytes. Previous studies have shown that the expression of large amounts of GFAP by muller cells only occurs under conditions of retinal degeneration, detachment, or similar pathological conditions which disrupt communication between the retina and the brain[19-23].

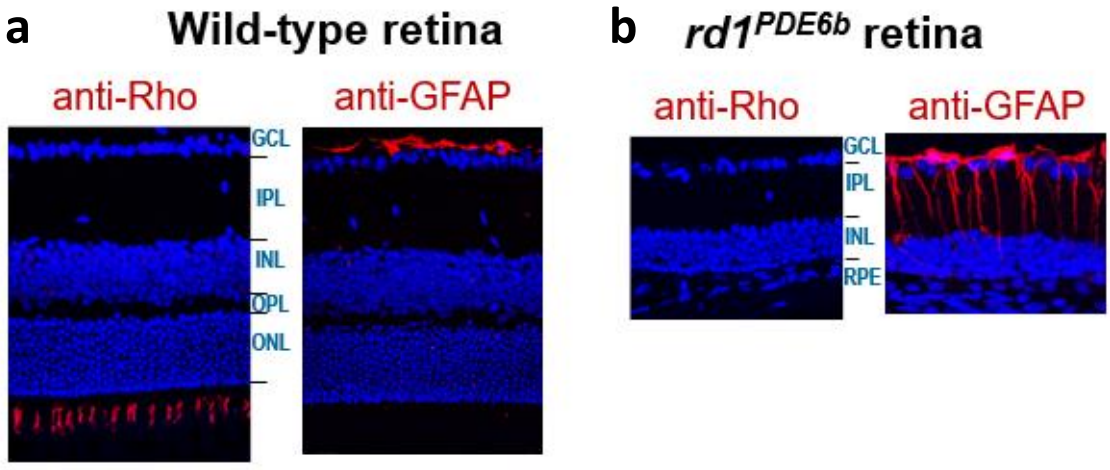


**Figure 7.** Loss of rod photoreceptor cells and significant increase of GFAP expression in the *rd1* mouse. Immuno-labeling with anti-Rho (red) and anti-GFAP (red), counter-staining with a nuclei dye DAPI (blue) in cross-sections of **(a)** wild-type retina and **(b)** the *rd1* retina.

**Pathological Changes of Vasculature in the *rd10* mouse**

Confocal microscopy images of flat-mounted *rd10* mouse retina at four weeks, labeled with anti-CD144, showed a relatively well-developed vascular plexus in the intermediate and deep layers (see Fig. 8). Substantial vasculature are present in the intermediate and deep plexuses (see right panels), compared to the *rd1* retina (middle panels), although the densities of the blood vessels in these two plexuses are reduced in

the *rd10* retina compared to the wild-type (left panels). Because photoreceptor degeneration in the *rd10* occurs in the late stages of retinal development and, since the onset of the degeneration is much slower than the *rd1*, most photoreceptors in the *rd10* retina survive during retinal development (see Introduction). A comparison of vascular degenerations in the *rd1* and *rd10* mouse clearly indicates a pattern in which there is less blood vessel loss in the retina with slower photoreceptor degeneration. Our results support the notion that the survival of photoreceptors and blood vessels in the diseased retina is highly correlated to each other during the progression of the disease.

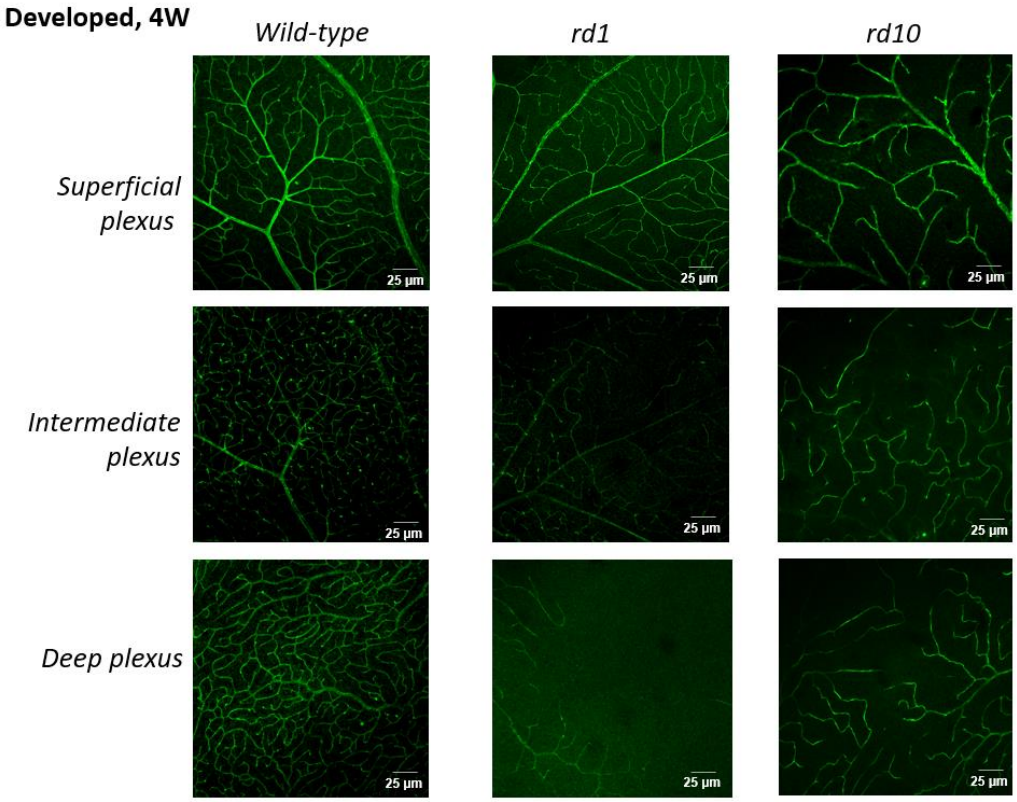


**Figure 8.** Confocal images of the superficial, intermediate, and deep plexuses of wild-type, *rd1*, and *rd10* mice at four weeks postnatal.

**Statistical Analyses of Vascular Degenerative Patterns**

While visualization is a necessary tool in the study of vasculature, there is still a need for a systematic characterization of changes in such tissues for ease of quantitative analysis that is reproducible and consistent across studies. We chose to use biologically relevant parameters related to vascular density in our characterization of vascular changes in the wild-type and *rd1* and *rd10* mouse retinas including: 1) vascular area fraction (the ratio of the area occupied by vasculature relative to the total area of the retinal image), 2) number of branches (points where vessels split into two), 3) number of junctions (points that connect two or more branches), and 4) junction to branch ratio. We compared the above parameters in *rd1* and *rd10* mice to the wild-type control at different post-developmental time points beginning at four weeks postnatal in the wild-type while the *rd1* and *rd10* mice were age-matched at 8 weeks postnatal. Overall, average vascular area fractions decreased in the *rd1* retinas compared to the wild-type by percentages (center, middle, and peripheral) of -49%, -48%, and -73% in the superficial plexus (SP), -73%, -59%, and -70% in the intermediate plexus (IP), and -70% , -70%, and -73% in the deep plexus (DP) (see Table 1 and 2). The results indicate that there is significant loss of blood vessels in the center, middle and peripheral regions of the diseased retinas. Average vascular area fraction was much smaller in the intermediate and deep plexus of *rd1* mice compared to the wild-type. The average number of branches and junctions in *rd1* mice reflected an overall decrease that was more pronounced in the intermediate and deep plexus as well. The average number of branches changed in the *rd1* retinas compared to the wild-type by percentages (center, middle, and peripheral) of +29%, -32%, and -32% in the SP, -71%, -70%, and -64% in the IP, and -72%, -56%, and -68% in the DP (see Table 1 and 2). The average number of junctions changed in the *rd1* retinas compared to

the wild-type by percentages (center, middle, and peripheral) of -13%, +25%, and -33% in the SP, -75%, -72%, and -77% in the IP, and -70%, -60%, and -56% in the DP (see Table 1 and 2). These results support the indication by our preliminary data that changes in the retinal vasculature in the *rd1* mouse model of retinal degeneration occur in a plexus-specific manner and are more pronounced in the intermediate and deep layers of the retina.

The *rd10* mice showed, to a lesser degree, similar changes in average vascular area fractions when compared to the wild-type mice. Overall, average vascular area fractions decreased in the *rd10* retinas compared to the wild-type by percentages (center, middle, and peripheral) of -27%, -9%, and -66% in the SP, -62%, -80%, and -67% in the IP, and -55%, -69%, and -73% in the DP (see Table 1 and 3). Once again, vascular area fractions seemed to decrease more in the intermediate and deep plexus. The average number of branches changed in the *rd10* retinas compared to the wild-type by percentages (center, middle, and peripheral) of +14%, -44%, and -31% in the SP, -71%, -82%, and -61% in the IP, and -69%, -68%, and -82% in the DP (see Table 1 and 3). The average number of junctions changed in the *rd10* retinas compared to the wild-type by percentages (center, middle, and peripheral) of -25%, 0%, and -33% in the SP, -72%, -88%, and -77% in the IP, and -80%, -70%, and -88% in the DP (see Table 1 and 3).

The results further indicate to a degree that early onset photoreceptor degeneration, such as that seen in the *rd1* mouse retina, influences a quicker and more drastic change in retinal vasculature and this change is more pronounced in the intermediate and deep plexuses of the retinal vascular network. In the *rd10* mouse, such

vascular changes may not be seen until after the late onset photoreceptor degeneration beginning after the fourth week of life. The junction to branch ratio of the vascular plexuses in the center, middle, and peripheral retina were variable but generally smaller in the rd1 and rd10 mice, reflecting the degeneration of vessels in the diseased retina, however, these changes did not seem to be plexus-specific as with average vascular area fractions, number of branches, and number of junctions. Our statistical analyses provide a scientific value for the imaging data describing vascular remodeling in retinal degenerative disease.

**WT Center Retina Analysis**

| mouse type/plexus layer | | vascular area fraction | number of branches | number of junctions | Junction to Branch Ratio |
|---|---|---|---|---|---|
| wild-type-SP | Mean | .117 | 7.000 | 2.667 | 2.778 |
| | N | 3.000 | 3.000 | 3.000 | 3.000 |
| | Std. Deviation | .009 | 1.732 | .577 | 1.170 |
| wild-type-IP | Mean | .239 | 42.000 | 13.333 | 3.145 |
| | N | 3.000 | 3.000 | 3.000 | 3.000 |
| | Std. Deviation | .029 | 6.083 | 1.528 | .135 |
| wild-type-DP | Mean | .122 | 13.000 | 3.333 | 4.289 |
| | N | 3.000 | 3.000 | 3.000 | 3.000 |
| | Std. Deviation | .011 | 2.646 | 1.528 | 1.500 |

**WT Middle Retina Analysis**

| mouse type/plexus layer | | vascular area fraction | number of branches | number of junctions | Junction to Branch Ratio |
|---|---|---|---|---|---|
| wild-type-SP | Mean | .121 | 8.333 | 1.333 | 6.667 |
| | N | 3.000 | 3.000 | 3.000 | 3.000 |
| | Std. Deviation | .002 | 2.082 | .577 | 2.082 |
| wild-type-IP | Mean | .297 | 33.333 | 10.667 | 3.137 |
| | N | 3.000 | 3.000 | 3.000 | 3.000 |
| | Std. Deviation | .044 | 5.774 | 2.082 | .174 |
| wild-type-DP | Mean | .135 | 11.333 | 3.333 | 3.400 |
| | N | 3.000 | 3.000 | 3.000 | 3.000 |
| | Std. Deviation | .000 | .000 | .000 | .000 |

**WT Peripheral Retina Analysis**

| mouse type/plexus layer | | vascular area fraction | number of branches | number of junctions | Junction to Branch Ratio |
|---|---|---|---|---|---|
| wild-type-SP | Mean | .174 | 9.333 | 2.000 | 5.833 |
| | N | 3.000 | 3.000 | 3.000 | 3.000 |
| | Std. Deviation | .009 | .577 | 1.000 | 3.686 |
| wild-type-IP | Mean | .241 | 26.667 | 8.000 | 3.321 |
| | N | 3.000 | 3.000 | 3.000 | 3.000 |
| | Std. Deviation | .021 | 4.509 | 1.000 | .158 |
| wild-type-DP | Mean | .184 | 14.667 | 3.000 | 7.278 |
| | N | 3.000 | 3.000 | 3.000 | 3.000 |
| | Std. Deviation | .018 | 4.726 | 2.646 | 5.073 |

**Table 1.** Comparison of means of the following averaged parameters in imaging analysis of the retinal trilaminar vascular network in wild-type (WT) mice: vascular area fraction, number of branches, number of junctions, and junction to branch ratio. WT: n=9, regions of interest defined at 250 $\mu m^2$, age: 4W. SP: Superficial Plexus, IP: Intermediate Plexus, DP: Deep Plexus.

**rd1 Center Retina Analysis**

| mouse type/plexus layer | | vascular area fraction | number of branches | number of junctions | Junction to Branch Ratio |
|---|---|---|---|---|---|
| rd1-SP | Mean | .060 | 9.000 | 2.333 | 3.944 |
| | N | 3.000 | 3.000 | 3.000 | 3.000 |
| | Std. Deviation | .007 | 1.000 | .577 | .585 |
| rd1-IP | Mean | .064 | 12.333 | 3.333 | 3.957 |
| | N | 3.000 | 3.000 | 3.000 | 3.000 |
| | Std. Deviation | .015 | 3.215 | 1.528 | .934 |
| rd1-DP | Mean | .037 | 3.667 | 1.000 | 3.667 |
| | N | 3.000 | 3.000 | 3.000 | 3.000 |
| | Std. Deviation | .008 | .577 | .000 | .577 |

**rd1 Middle Retina Analysis**

| mouse type/plexus layer | | vascular area fraction | number of branches | number of junctions | Junction to Branch Ratio |
|---|---|---|---|---|---|
| rd1-SP | Mean | .063 | 5.667 | 1.667 | 3.444 |
| | N | 3.000 | 3.000 | 3.000 | 3.000 |
| | Std. Deviation | .007 | 3.786 | 1.155 | .509 |
| rd1-IP | Mean | .091 | 10.000 | 3.000 | 3.289 |
| | N | 3.000 | 3.000 | 3.000 | 3.000 |
| | Std. Deviation | .006 | 6.557 | 2.000 | .342 |
| rd1-DP | Mean | .041 | 5.000 | 1.333 | 3.833 |
| | N | 3.000 | 3.000 | 3.000 | 3.000 |
| | Std. Deviation | .001 | 2.000 | .577 | 1.041 |

**rd1 Peripheral Retina Analysis**

| mouse type/plexus layer | | vascular area fraction | number of branches | number of junctions | Junction to Branch Ratio |
|---|---|---|---|---|---|
| rd1-SP | Mean | .047 | 6.333 | 1.333 | 5.000 |
| | N | 3.000 | 3.000 | 3.000 | 3.000 |
| | Std. Deviation | .010 | 2.082 | .577 | 1.732 |
| rd1-IP | Mean | .072 | 9.667 | 2.667 | 3.944 |
| | N | 3.000 | 3.000 | 3.000 | 3.000 |
| | Std. Deviation | .010 | 4.509 | 1.528 | .918 |
| rd1-DP | Mean | .050 | 4.667 | 1.333 | 3.500 |
| | N | 3.000 | 3.000 | 3.000 | 3.000 |
| | Std. Deviation | .017 | 2.082 | .577 | .500 |

**Table 2.** Comparison of means of the following averaged parameters in imaging analysis of the retinal trilaminar vascular network in *rd1* mice: vascular area fraction, number of branches, number of junctions, and junction to branch ratio. *rd1*: n=9, regions of interest defined at 250 $\mu m^2$, age: 8W. SP: Superficial Plexus, IP: Intermediate Plexus, DP: Deep Plexus.

**rd10 Center Retina Analysis**

| mouse type/plexus layer | | vascular area fraction | number of branches | number of junctions | Junction to Branch Ratio |
|---|---|---|---|---|---|
| rd10-SP | Mean | .086 | 8.000 | 2.000 | 4.389 |
| | N | 3.000 | 3.000 | 3.000 | 3.000 |
| | Std. Deviation | .031 | 2.646 | 1.000 | 1.398 |
| rd10-IP | Mean | .092 | 12.333 | 3.667 | 3.300 |
| | N | 3.000 | 3.000 | 3.000 | 3.000 |
| | Std. Deviation | .014 | 5.686 | 1.528 | .265 |
| rd10-DP | Mean | .055 | 4.000 | .667 | 3.333 |
| | N | 3.000 | 3.000 | 3.000 | 3.000 |
| | Std. Deviation | .041 | 2.000 | .577 | 3.055 |

**rd10 Middle Retina Analysis**

| mouse type/plexus layer | | vascular area fraction | number of branches | number of junctions | Junction to Branch Ratio |
|---|---|---|---|---|---|
| rd10-SP | Mean | .110 | 4.667 | 1.333 | 3.500 |
| | N | 3.000 | 3.000 | 3.000 | 3.000 |
| | Std. Deviation | .045 | 2.082 | .577 | .500 |
| rd10-IP | Mean | .060 | 6.000 | 1.333 | 4.500 |
| | N | 3.000 | 3.000 | 3.000 | 3.000 |
| | Std. Deviation | .029 | 2.646 | .577 | .500 |
| rd10-DP | Mean | .042 | 3.667 | 1.000 | 2.000 |
| | N | 3.000 | 3.000 | 3.000 | 3.000 |
| | Std. Deviation | .038 | 2.082 | 1.000 | 1.732 |

**rd10 Peripheral Retina Analysis**

| mouse type/plexus layer | | vascular area fraction | number of branches | number of junctions | Junction to Branch Ratio |
|---|---|---|---|---|---|
| rd10-SP | Mean | .077 | 6.333 | 1.333 | 5.000 |
| | N | 3.000 | 3.000 | 3.000 | 3.000 |
| | Std. Deviation | .019 | 2.082 | .577 | 1.732 |
| rd10-IP | Mean | .079 | 10.333 | 2.667 | 3.944 |
| | N | 3.000 | 3.000 | 3.000 | 3.000 |
| | Std. Deviation | .028 | 1.528 | .577 | .585 |
| rd10-DP | Mean | .049 | 2.667 | .667 | 2.000 |
| | N | 3.000 | 3.000 | 3.000 | 3.000 |
| | Std. Deviation | .016 | .577 | .577 | 1.732 |

**Table 3.** Comparison of means of the following averaged parameters in imaging analysis of the retinal trilaminar vascular network in *rd10* mice: vascular area fraction, number of branches, number of junctions, and junction to branch ratio. *rd10*: n=9, regions of interest defined at 250 $\mu m^2$, age: 8W. SP: Superficial Plexus, IP: Intermediate Plexus, DP: Deep Plexus.

Altogether, our results provide support for the use of certain vascular density parameters, such as vascular area fraction, as indications of vascular changes during conditions of retinal degeneration in the *rd1*/*rd10* mice. Based on our findings, the *rd10* mouse may be more accessible to studies based on intervention at specific time points as the *rd10* mouse represents a slow model of retinal degeneration. The *rd1* mouse exhibits fast changes to the vasculature in response to an earlier onset of photoreceptor degeneration.

# DISCUSSION

Due to the fact that mice exhibit a postnatal development of the retinal vasculature, these animals are ideal for studying vascular development and degeneration in response to photoreceptor cell death. The mouse retina has been the ideal choice for researchers studying the pathogenesis of retinal degenerative disease, partly due to the large body of genetically altered mouse models that are available[24,25]. The ready availability of open-source imaging software coupled with easily accessible analytical plugins resulting from collaborations across disciplines has also contributed to our understanding of vascular changes in retinal degenerative disease. This technology may help us to discover novel therapies for patients suffering from retinal degenerative diseases like retinitis pigmentosa. In our study, we utilized the open-source ImageJ analysis software (FIJI) in order to process and quantitatively analyze the retinal vasculature in its three layers. We chose to use single-plexus analysis and comparisons based off previous studies that reported a more accurate representation of three-dimensional retinal vasculature in single-plexus versus whole tissue analysis[3].

## Photoreceptor Degeneration Influences Vascular Development in RD Mice

Two mouse models of retinal degeneration were utilized in this study, the *rd1* and *rd10* mice which carry mutations in the photoreceptor cGMP phosphodiesterase 6b (*pde6b*) gene. What separates these two similar models is the time frame during which photoreceptor degeneration occurs. Confocal imaging studies revealed that the *rd1* mouse

exhibits the loss of photoreceptor cells, specifically rods, around p14 or earlier, whereas photoreceptor degeneration in *rd10* mice does not typically occur until after the fourth postnatal week when vascular development is essentially complete[26]. At p7, we observed that the development of the superficial vascular plexus in wild-type and *rd1* mice was normal. This occurrence is well documented in other mouse models of retinal degeneration since, even in fast models of retinal degeneration like the *rd1* mouse, superficial plexus development occurs prior to complete photoreceptor degeneration[27,28]. At p14, the intermediate and deep vascular plexuses of the *rd1* mouse retina were noticeably less developed than its wild-type counterpart. Retinal cross-sections with anti-Rhodopsin and DAPI nuclei staining also revealed a loss of rod photoreceptors coupled with some thinning of the outer nuclear layer and increased expression of GFAP which is typically associated with pathological conditions in the retina[29,30]. By p21, the *rd1* mouse retina is nearly void of all vasculature in the intermediate and deep plexuses whereas the wild-type retina has developed a complex network of vasculature in these layers. Since the superficial vascular plexus branches off the central retinal artery, the plexus persists even after most of the photoreceptors are lost. Our results led us to conclude that early onset photoreceptor degeneration disrupts the development of retinal vasculature in the *rd1* mouse, specifically in the intermediate and deep vascular plexuses. Such information may prove to be especially useful to studies centered on intervention during development of the retina. The *rd10* retinas did not exhibit developmental changes in the vasculature, however, we found some post-developmental changes that coincide with the time frame during which *rd10* mice experience photoreceptor degeneration.

Given the later onset of photoreceptor degeneration in *rd10* mice, we expected to see relatively normal vascular development up until at least p21, at which point the final intermediate plexus should finish developing. Confocal imaging done at four weeks postnatal showed a relatively well-developed intermediate and deep plexus in the *rd10* retina with a normal superficial plexus. The *rd10* mouse retina serves as an important comparison point for delineating the influence of photoreceptor degeneration on vascular development. While the *rd1* mouse retina begins to exhibit vascular degeneration prior to normal development, the *rd10* mouse retina may only exhibit vascular changes after development of the vasculature has completed. In order to quantitatively compare the differences in vascular plexus formation in the RD and wild-type mice, we chose parameters that are biologically relevant to vascular density.

**Statistical Analyses of Vasculature in Developing and Adult *rd1* and *rd10* Retina**

Vascular density in the retinal trilaminar network has been shown to be affected under conditions of retinal degeneration and is associated with tissue oxygenation and nutrition[4,26,27]. In this study we measured vascular area fraction, number of branches, number of junctions, and junction to branch ratios in order to characterize the vascular changes that occur following photoreceptor degeneration in the *rd1* and *rd10* mouse. We describe a relatively normal development of the superficial vascular plexus in both the wild-type and retinal degenerative mice groups, but a marked decrease in average vascular area fraction in the intermediate and deep plexus of the *rd1* mouse. The *rd10* mouse exhibited normal vascular development until the end of the fourth week where it began to lose vascular density in the intermediate and deep plexus as evidenced by a much smaller vascular area fraction. These findings are consistent with data from studies

performed on similar animal models[31]. Physiologically, the degeneration of vasculature, particularly in the intermediate and deep plexuses of RD retina, seem to hinder the spread of vessels via branching and the formation of junctions. While the junction to branch ratios of the SP, IP, and DP in the center, middle, and peripheral retina did not reveal any clear findings in regard to vascular development, the average number of branches and junctions were found to be much lower in the IP and DP of the diseased retina. The results lead us to theorize that vascular changes are correlated to the onset of photoreceptor degeneration in the mouse retina.

The *rd1* and *rd10* mice represent fast and slow models of retinal degeneration, respectively. By systematically characterizing the vascular changes following photoreceptor degeneration in these mouse models using biologically relevant parameters, we offer insight into the time frame of disease processes that are unique to retinal degeneration. In the *rd1* mouse retina, photoreceptor degeneration begins within the first two weeks of life as evidenced by the labeling of anti-Rho and nuclear staining in retinal cross-sections throughout development (see Results). Conversely, photoreceptor degeneration in the rd10 mouse does not occur until much later after the development of the retinal vasculature is complete. We cite previous studies which show that the expression of opsins by cone outer segments in the rd10 retina persist through the 6$^{th}$ and 7$^{th}$ postnatal week. Our results indicate that photoreceptor survival is a key element for interventions directed at the rescue of retinal vasculature both before and after development. Attempts at understanding the mechanism of photoreceptor degeneration, relative to the development of the retinal vasculature, must be made in order to produce

successful interventions that mitigate or prevent the progression of retinal degeneration and subsequent loss of vision.

## Conclusion

The results of our study provide valuable insight into the nature of vascular changes that characterize retinal degenerative disease such as retinitis pigmentosa. While this study will likely extend our knowledge of the mechanisms underlying retinal degeneration, it remains an important challenge in treating these diseases. The long-term goal of this study is to open new avenues of research aimed at developing novel therapies for retinal degenerative disease. Future studies may look at strategies promoting blood vessel survival and protection in specific time points as potential therapies for mitigating retinal degeneration. The vascular system is critical for supplying oxygen and nutrients to tissues, especially those with high metabolic demand as seen in the retina. Given the correlation between vascular changes and photoreceptor degeneration, approaches to therapies for retinal degenerative disease must take into account the mechanisms of both events.

## Future Perspectives

Previous studies investigating the mechanisms of photoreceptor degeneration have typically relied on a single, apoptotic cell death mechanism[32,33]. However, given the remarkable parallelism between photoreceptor cell loss and vascular degeneration highlighted in this study, there is potential value in targeting mechanisms which are related to vascular function. One such avenue of research may look at molecular pathways that modulate oxidative stress and inflammation. It has been documented that,

in humans, retinal cells are consistently exposed to oxidative stress as a result of normal physiological conditions such as light exposure and the normal activity of visual signal transduction pathways[34]. In pathological conditions, such as retinal degeneration, there is an imbalance between pro-oxidant signaling activity that generates reactive oxygen species and anti-oxidant activity that serves to eliminate them. Thus, this imbalance leads to excess oxidative stress and subsequent inflammation. Such conditions lead to the altered expressions of certain genes that modulate endothelial cell function in vascular systems.

Vascular endothelial growth factor (VEGF) and platelet derived endothelial cell growth factor (PDGF) are two examples of genes that exhibit altered expression under pathological conditions of oxidative stress and inflammation[36]. While the exact actions of VEGF and PDGF under conditions of retinal degeneration are not completely understood, there is reason to believe that both of these endothelial cell growth factors may be key components in understanding the nature of vascular remodeling and degeneration in response to photoreceptor cell death. Considering that VEGF and PDGF play major roles in the formation of primary vasculature and subsequent growth and proliferation of vascular endothelial cells, there is a potential avenue of study concerning the actions of molecular pathways involving these growth factors during retinal degeneration. This study aims to support future endeavors into the role of such elements in mitigating retinal degeneration and subsequent, irreversible vision loss by providing a practical and consistent method of studying the vascular architecture via three-dimensional models in conjunction with a quantitative analysis of vascular changes that can be reproduced and compared across studies in an efficient manner.

REFERENCES


1. Zhang, Q. (2016). Retinitis pigmentosa: progress and perspective. *The Asia-Pacific Journal of Ophthalmology*, *5*(4), 265-271.

2. Ferrari, S., Di Iorio, E., Barbaro, V., Ponzin, D., S Sorrentino, F., & Parmeggiani, F. (2011). Retinitis pigmentosa: genes and disease mechanisms. *Current genomics*, *12*(4), 238-249.

3. Rust, R., Grönnert, L., Dogançay, B., & Schwab, M. E. (2019). A revised view on growth and remodeling in the retinal vasculature. *Scientific reports*, *9*(1), 1-9.

4. Hughes, S., Yang, H., & Chan-Ling, T. (2000). Vascularization of the human fetal retina: roles of vasculogenesis and angiogenesis. *Investigative ophthalmology & visual science*, *41*(5), 1217-1228.

5. Fruttiger M. (2007). Development of the retinal vasculature. *Angiogenesis*, *10*(2), 77–88.

6. Fruttiger, M. (2002). Development of the mouse retinal vasculature: angiogenesis versus vasculogenesis. *Investigative ophthalmology & visual science*, *43*(2), 522-527.

7. McLeod, D. S., Hasegawa, T., Prow, T., Merges, C., & Lutty, G. (2006). The initial fetal human retinal vasculature develops by vasculogenesis. *Developmental*

*dynamics: an official publication of the American Association of Anatomists*, *235*(12), 3336-3347.

8. Xu, Q., Wang, Y., Dabdoub, A., Smallwood, P. M., Williams, J., Woods, C., Kelley, M. W., Jiang, L., Tasman, W., Zhang, K., & Nathans, J. (2004). Vascular development in the retina and inner ear: control by Norrin and Frizzled-4, a high-affinity ligand-receptor pair. *Cell*, *116*(6), 883–895.

9. Ye, X., Wang, Y., & Nathans, J. (2010). The Norrin/Frizzled4 signaling pathway in retinal vascular development and disease. *Trends in molecular medicine*, *16*(9), 417-425.

10. Junge, H. J., Yang, S., Burton, J. B., Paes, K., Shu, X., French, D. M., ... & Ye, W. (2009). TSPAN12 regulates retinal vascular development by promoting Norrin-but not Wnt-induced FZD4/β-catenin signaling. *Cell*, *139*(2), 299-311.

11. Pittler, S. J., & Baehr, W. (1991). Identification of a nonsense mutation in the rod photoreceptor cGMP phosphodiesterase beta-subunit gene of the rd mouse. *Proceedings of the National Academy of Sciences*, *88*(19), 8322-8326.

12. Lem, J., Flannery, J., Li, T., Applebury, M., Farber, D., & Simon, M. (1992). Retinal Degeneration is Rescued in Transgenic rd Mice by Expression of the cGMP Phosphodiesterase β Subunit. *Proceedings of the National Academy of Sciences of the United States of America*, *89*(10), 4422-4426.

13. Nishiguchi, K. M., Carvalho, L. S., Rizzi, M., Powell, K., kleine Holthaus, S. M., Azam, S. A., ... & Smith, A. J. (2015). Gene therapy restores vision in *rd1* mice after removal of a confounding mutation in Gpr179. *Nature communications*, *6*(1), 1-10.

14. Yang, J., Nan, C., Ripps, H., & Shen, W. (2015). Destructive changes in the neuronal structure of the FVB/N mouse retina. *PLoS One*, *10*(6), e0129719.

15. McLaughlin, M. E., Sandberg, M. A., Berson, E. L., & Dryja, T. P. (1993). Recessive mutations in the gene encoding the β–subunit of rod phosphodiesterase in patients with retinitis pigmentosa. *Nature genetics*, *4*(2), 130-134.

16. Chang, B., Hawes, N. L., Pardue, M. T., German, A. M., Hurd, R. E., Davisson, M. T., ... & Boatright, J. H. (2007). Two mouse retinal degenerations caused by missense mutations in the β-subunit of rod cGMP phosphodiesterase gene. *Vision research*, *47*(5), 624-633

17. Barhoum, R., Martinez-Navarrete, G., Corrochano, S., Germain, F., Fernández-Sánchez, L., De la Rosa, E. J., ... & Cuenca, N. (2008). Functional and structural modifications during retinal degeneration in the *rd10* mouse. *Neuroscience*, *155*(3), 698-713.

18. Li, B., Gografe, S., Munchow, A., Lopez-Toledano, M., Pan, Z. H., & Shen, W. (2019). Sex-related differences in the progressive retinal degeneration of the rd10 mouse. *Experimental eye research*, *187*, 107773.

19. Eisenfeld, A. J., Bunt-Milam, A. H., & Sarthy, P. V. (1984). Müller cell expression of glial fibrillary acidic protein after genetic and experimental photoreceptor

degeneration in the rat retina. *Investigative ophthalmology & visual science*, *25*(11), 1321-1328.

20. Erickson, P. A., Fisher, S. K., Guérin, C. J., Anderson, D. H., & Kaska, D. D. (1987). Glial fibrillary acidic protein increases in Müller cells after retinal detachment. *Experimental eye research*, *44*(1), 37-48.

21. Cao, W., Li, F., Steinberg, R. H., & Lavail, M. M. (2001). Development of normal and injury-induced gene expression of aFGF, bFGF, CNTF, BDNF, GFAP and IGF-I in the rat retina. *Experimental eye research*, *72*(5), 591-604.

22. Sarthy, P. V., Fu, M., & Huang, J. (1991). Developmental expression of the glial fibrillary acidic protein (GFAP) gene in the mouse retina. *Cellular and molecular neurobiology*, *11*(6), 623-637.

23. Wu, K. H. C., Madigan, M. C., Billson, F. A., & Penfold, P. L. (2003). Differential expression of GFAP in early v late AMD: a quantitative analysis. *British journal of ophthalmology*, *87*(9), 1159-1166.

24. Liu, H., Tang, J., Du, Y., Saadane, A., Tonade, D., Samuels, I., ... & Kern, T. S. (2016). Photoreceptor cells influence retinal vascular degeneration in mouse models of retinal degeneration and diabetes. *Investigative ophthalmology & visual science*, *57*(10), 4272-4281.

25. Chang, B. (2012). Mouse models for studies of retinal degeneration and diseases. In *Retinal Degeneration* (pp. 27-39). Humana Press, Totowa, NJ.

26. Phillips, M. J., Otteson, D. C., & Sherry, D. M. (2010). Progression of neuronal and synaptic remodeling in the *rd10* mouse model of retinitis pigmentosa. *Journal of Comparative Neurology*, *518*(11), 2071-2089.

27. Fernández-Sánchez, L., Esquiva, G., Pinilla, I., Lax, P., & Cuenca, N. (2018). Retinal vascular degeneration in the transgenic p23h rat model of retinitis pigmentosa. *Frontiers in neuroanatomy*, *12*, 55.

28. Yang, J., Nan, C., Ripps, H., & Shen, W. (2015). Destructive changes in the neuronal structure of the FVB/N mouse retina. *PLoS One*, *10*(6), e0129719.

29. Hsiao, C. C., Hsu, H. M., Yang, C. M., & Yang, C. H. (2019). Correlation of retinal vascular perfusion density with dark adaptation in diabetic retinopathy. *Graefe's Archive for Clinical and Experimental Ophthalmology*, *257*(7), 1401-1410.

30. Kim, T. H., Son, T., Lu, Y., Alam, M., & Yao, X. (2018). Comparative optical coherence tomography angiography of wild-type and *rd10* mouse retinas. *Translational vision science & technology*, *7*(6), 42-42.

31. Pennesi, M. E., Nishikawa, S., Matthes, M. T., Yasumura, D., & LaVail, M. M. (2008). The relationship of photoreceptor degeneration to retinal vascular development and loss in mutant rhodopsin transgenic and RCS rats. *Experimental eye research*, *87*(6), 561-570.

32. Trifunovic, D., Sahaboglu, A., Kaur, J., Mencl, S., Zrenner, E., Ueffing, M., ... & Paquet-Durand, F. (2012). Neuroprotective strategies for the treatment of inherited photoreceptor degeneration. *Current molecular medicine*, *12*(5), 598-612.

33. Chang, G. Q., Hao, Y., & Wong, F. (1993). Apoptosis: Final common pathway of photoreceptor death in rd, rds, and mutant mice. *Neuron, 11*(4), 595-605.